

EXPERIMENTAL STRESS ANALYSIS OF TWO WHEELER CONNECTING ROD USING PHOTOELASTICITY

Akbar H Khan¹, Dr. Dhananjay R Dolas², Prof. M.M.Mirza³

¹. PG Student, Mechanical Department, MGM's JNEC Aurangabad, MH India.

². Associate Professor, Mechanical Department, MGM's JNEC Aurangabad, MH India.

³. Assistant Professor, Mechanical Department, RIT Islampur, Sangli, MH India.

ABSTRACT

The connecting rod is the most relevant parts of an automotive engine. The connecting rod is subjected to an extremely complex state of loading. High compressive and tensile loads are due to the combustion and connecting rod's mass of inertia respectively. The objective of this research is to investigate the failure analysis of the two wheeler connecting rod so that Stress analysis is carried out to determine the Maximum principle stresses in the present design of connecting rod for the given compressive and tensile loading conditions using the FEA Software Ansys 15.0. The comparison and the verification of the results obtained in FEA is done experimentally by the method of Photoelasticity. The method of Photoelasticity includes the casting of Photoelastic sheet using Araldite Resin AY103 and Hardener HY991, and the model is prepared using Photoelastic sheet as well as calibration of the sheet is done to determine the material fringe value.

Keywords: - Connecting rod, Photoelasticity, Two Wheeler, FEA, Araldite Resin, and Ansys.

1.0 INTRODUCTION

The automobile engine connecting rod is a high volume production, critical component. It connects Reciprocating piston to rotating crankshaft, transmitting the thrust of the piston to the crankshaft. Every vehicle that uses an internal combustion engine requires at least one connecting rod depending upon the number of cylinders in the engine. Beside these points Samand engine is national engine of Iran and also Samand is one of numerous vehicles of Iran. According to above reasons, it is only logical that optimization of the connecting rod for its weight or volume will result in large-scale savings. It can also achieve the objective of reducing the weight of the engine component, thus reducing inertia loads, reducing engine weight and improving engine performance and fuel economy.

The connecting rod is subjected to a complex state of loading. It undergoes high cyclic loads of the order of 108 to 109 cycles, which range from high compressive loads due to combustion, to high tensile loads due to inertia. Therefore, durability of this component is of critical importance. Due to these factors,

The cyclic loading is very important factor in design of connecting rod. The increase in cross section of connecting rod effects the overall balancing of Engine. If the mass of connecting rod increases than the overall crankshaft design will get affected as a rotary mass gets increase the crankshaft balancing requirement also get increases. Now if the balancing requirement of engine gets increase than the Engine overall vibration gets increase which leads to failure of it component. To keep a fine balance between connecting rod weight and the crankshaft design optimization of weight is required. Although crankshaft design is out of the scope of the paper normally the overall design of engine needs to be considered in designing of connecting rod for engine.

1.1 Function of connecting rod

The function of connecting rod is to transmit the thrust of the piston to the crankshaft. Figure 1.1 shows the role of connecting rod from reciprocating motion into rotary motion. A four-stroke engine is the most common type. The four strokes are intake, compression, power, and exhaust. Each stroke requires approximately 180 degrees of crankshaft rotation, so the complete cycle would take 720 degrees. Each stroke plays a very important role in the combustion process as shown in Figure 1.1. In the intake cycle, while the piston moves downward, one of the valves open. This creates a vacuum, and an air-fuel mixture is sucked into the chamber, see Figure 1.1 (a). During the second stroke compression occurs. In compression both valves are closed, and the piston moves upward and thus creates a pressure on the piston, see Figure 1.1 (b). The next stroke is power. During this process the compressed air-fuel mixture is ignited with a spark, causing a tremendous pressure as the fuel burns. The forces exerted by piston transmitted through the connecting rod moves the crankshaft; see Figure 1.1 (c). Finally, the exhaust stroke occurs. In this stroke, the exhaust valve open, as the piston moves back upwards, it forces all the air out of the chamber and thus which completes the cycle of crankshaft rotation, see Figure 1.1 (d).

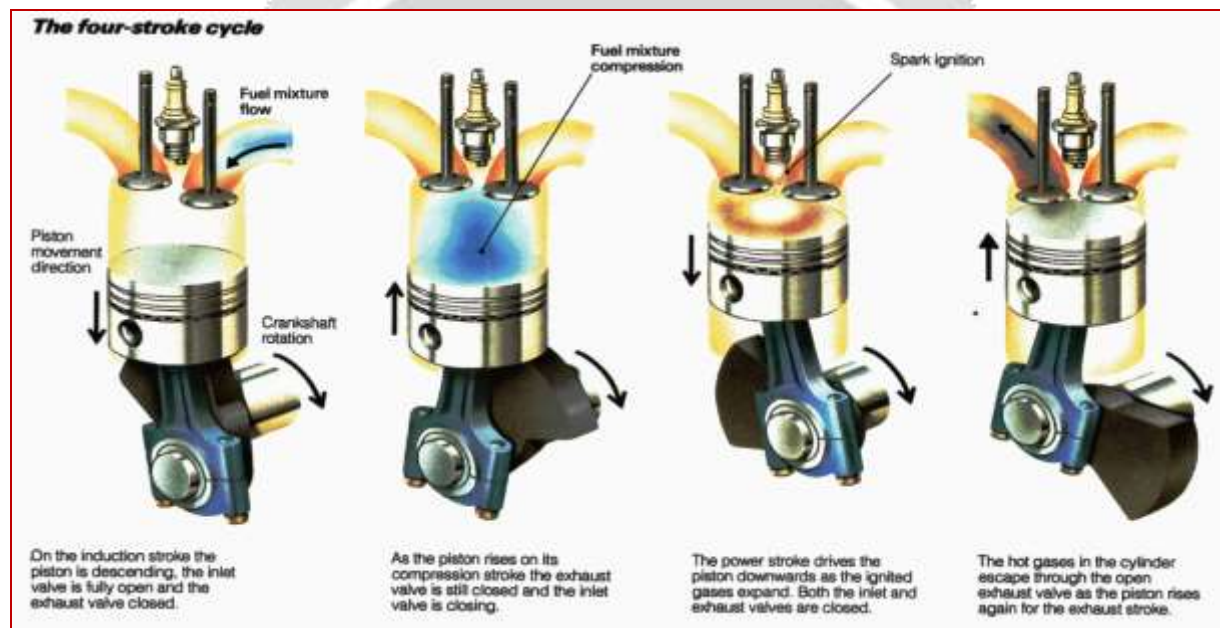


Figure: 1.1. Function of connecting rod in four stroke IC engine

2.0 LITURATURE SURVEY

The connecting rod has been the topic of research for different aspects such as production technology, materials, performance simulation, fatigue, etc. For the current study, it was necessary to investigate finite element modeling techniques, optimization techniques, developments in production technology, new materials, fatigue modeling, and manufacturing cost analysis. This brief literature survey reviews some of these aspects.

Ishida et al. [1995] measured the stress variation at the column center and column bottom of the connecting rod, as well as the bending stress at the column center. It is been observed that at the higher engine speeds, the peak tensile stress does not occur at 360o crank angle or top dead center. It was also observed that the R ratio varies with location, and at a given location it also varies with the engine speed. The maximum bending stress magnitude over the entire cycle (0o to 720o crank Angle) at 12000 rev/min, at the column center was found to be about 25% of the peak tensile stress over the same cycle.

Hyungyil Lee et al [2010] Buckling sensitivity of a connecting rod to the shank sectional area reduction, In this study a procedure of estimating critical buckling stress for a connecting rod was

suggested by using FEA with actual loading and boundary conditions. The validity of the buckling analysis was demonstrated by analyzing the sensitivity in yield, fatigue and buckling, which are important guides for weight reduction design of connecting rod shank.

Y.Liu et al [2011] Microstructures and mechanical properties of titanium alloy connecting rod made by powder forging process, in this research A new powder metallurgy titanium alloy connecting rod formed by a powder forging process was successfully developed with the help of a pre-processing simulation using a commercial finite element software. The microstructures and the mechanical properties of the deformed material were evaluated. The results indicate that the microstructures of the crank pin end, fork part and piston pin end are lamellar $\alpha + \beta$ structures and the microstructure of shank is of through transus β modal phase. The tensile strength and elongation are much higher than those of the most widely used PF-11C50/60 steels, and can well meet the requirements of the connecting-rod industry.

O.P.Singh et al [2011] Spalling investigation of connecting rod, while working on a connecting rod A laboratory test set-up was developed to correlate and reproduce the field failures. The loads and boundary conditions obtained from the experiments were used in the finite element model of the connecting rod assembly. Results show high interfacial pressure and stresses near the junction of web and flange of the connecting rod. The modified design of the connecting rod shows significant reduction in the extreme pressure in FEM resulting in the significant enhancement of durability life in laboratory test. A discussion of the spalling problem has been provided leading to the connection of pick pressure and spalling phenomena.

Yongqi liu et al [2011] Finite Element Analysis of Pump Diesel Engine Connecting Rod, in this paper, with the ANSYS, stress distribution of pump diesel engine connecting rod was analyzed by using 3D finite element method. The results show that the oil-hole of small end of connecting rod shank is the exposed destructive positions at maximum compression condition and maximum stretch condition. Maximum stress value is 371 MPa at maximum compression condition. Maximum deformation value is 0.149mm. Maximum stress value is 69.4MPa at maximum stretch condition. Maximum deformation value is 0.0168mm

2.1 Objective

The objective of this research is to investigate the failure analysis of the two wheeler connecting rod so that Stress analysis is carried out to determine the Maximum principle stresses in the present design of connecting rod for the given compressive and tensile loading conditions using the FEA Software Ansys 15.0. The comparison and the verification of the results obtained in FEA is done experimentally by the method of Photoelasticity and while doing the analysis the most critical area is considered where the failure of connecting occurs.

3.0 STRESS ANALYSIS OF CONNECTING ROD USING FEA.

Connecting rod specimen was modeled by taking the designed parameter of specimen and then by using the creo parameter 2.0 software solid modeling has done which is shown in Figure: 3.1 And saved within this program in *.IGES format. The model is imported in Ansys and then the mechanical characteristics of the connecting rod specimen are applied.

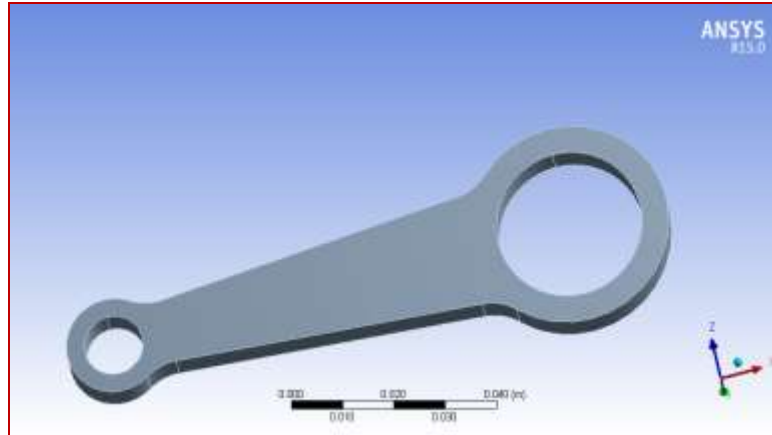


Figure: 3.1. Creo model of connecting rod specimen

3.1. Meshing

Here Meshing element chooses is 10 nodes named Solid187 as shown in figure: 2.2 First convergences was checked by finding deformation against different element size then plotting graph of deformation versus no of elements. Here element size is found out to be 2mm for working in convergence zone. Total No of element was 13403 and Nodes were 23962.

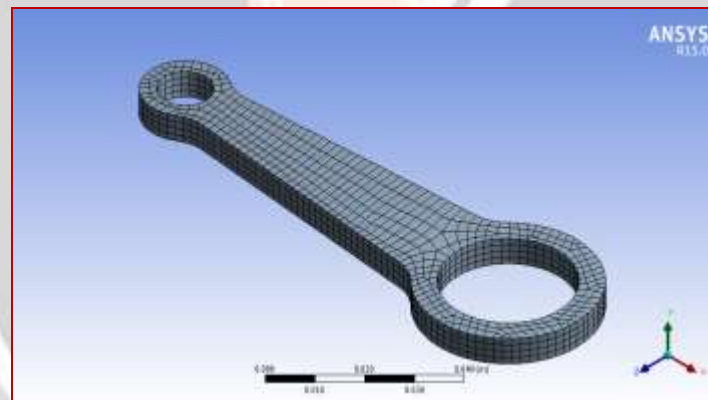
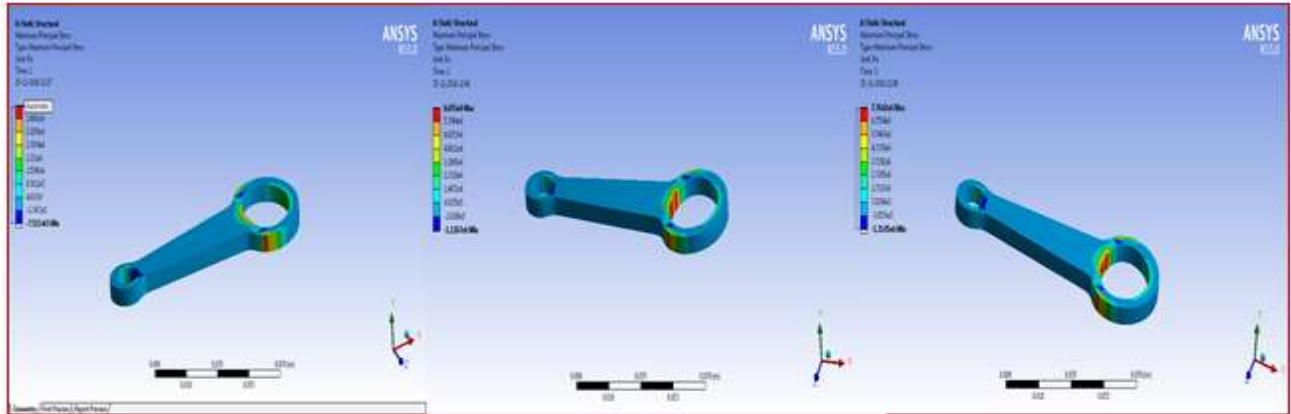


Figure: 3.2. Meshed model of connecting rod specimen

3.2. Loading and Boundary conditions

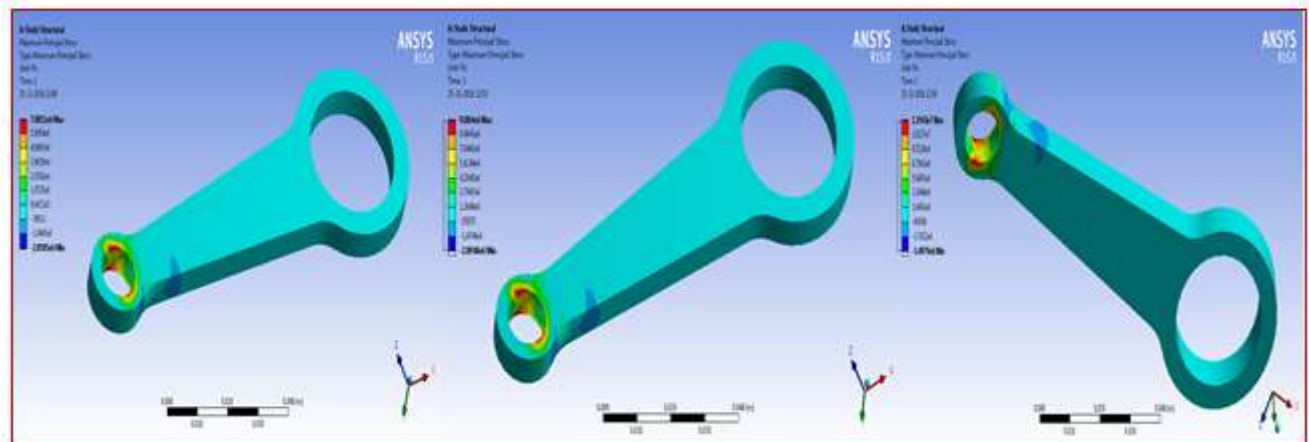
In this study one connecting rod specimen model is analyzed at different loads and finite element analysis for both compressive and tensile loads are conducted. Two cases are analyzed for each case, one with load applied at the big end and restrained at the small end of specimen, and the other with load applied at the small end and restrained at the big end. In the analysis carried out, the axial loads were 687 N, 834N and 981N in both compressive and tensile loading.

When a compressive load of 687N, 834N, and 981N is applied on big end of the specimen and small end is kept constant the maximum principle stress is generated on big end



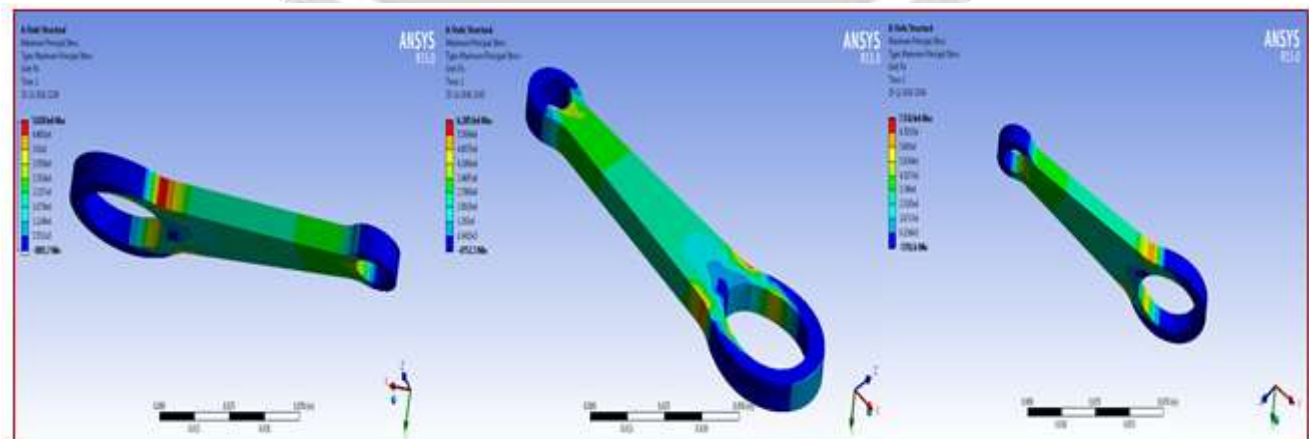
Figure; 3.3 maximum Principle Stress on big end is 4.43 Mpa, 6.65 Mpa, 7.76 Mpa.

When a compressive load of 687N, 834N, and 981N is applied on small end of the specimen and big end is kept constant the maximum principle stress is generated on big end



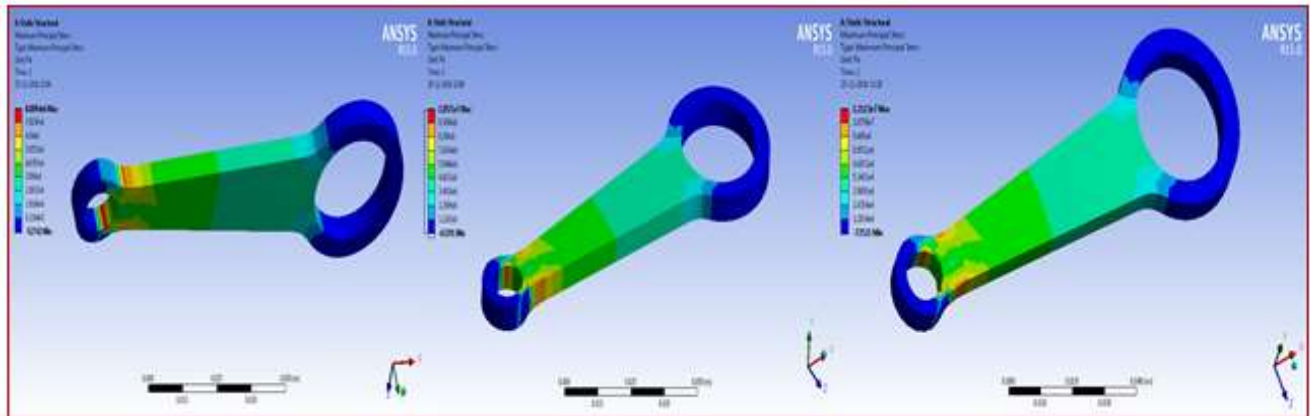
Figure; 3.4 maximum Principle Stress on big end is 7.01 Mpa, 9.88 Mpa, 11.94 Mpa.

When a tensile load of 687N, 834N, and 981N is applied on big end of the specimen and small end is kept constant the maximum principle stress is generated on big end



Figure; 3.5 maximum Principle Stress on big end is 5.02 Mpa, 6.28 Mpa, 7.54 Mpa.

When a tensile load of 687N, 834N, and 981N is applied on small end of the specimen and big end is kept constant the maximum principle stress is generated on big end.



Figure; 3.6 maximum Principle Stress on big end is 8.80 Mpa, 10.57 Mpa, 12.11 Mpa.

Table: 3.1. Comparative results of connecting rod specimen by finite element analysis

Applied Load (P) (N)	Maximum Principle Stress (MPa)			
	Compressive		Tensile	
	Big end	Small end	Big end	Small end
687	4.43	7.001	5.02	8.80
834	6.65	9.88	6.28	10.54
981	7.76	11.94	7.54	12.11

4.0. EXPERIMENTAL STRESS ANALYSIS USING PHOTOELASTICITY

The Photoelastic model of two wheeler connecting rod with required specification is prepared using Araldite AY 103 and Hardener HY 991 using Photoelastic sheet and then experimentally stress analysis is carried out in SAE lab on experimental setup of Photoelastic stress analysis Equipment; For the analysis of two wheeler connecting rod the most critical area and the major stresses like compressive and tensile stress is considered The different dimensions of the connecting rod are taken. Three loads, 70kg, 85kg and 100kg are applied at the both ends of connecting rod under the compressive and tensile loading conditions. These stresses calculated experimentally by Photoelasticity.

While conducting an experiment on Photoelastic sheet material using Photoelasticity it is necessary to find out the material fringe value which is known as calibration of Photoelastic sheet. Then we can conduct the experiment on our model for stress analysis.

4.1. Calibration of Photoelastic sheet

Calibration of Photoelastic sheet is carried out to find material fringe order and is conducted using circular disc of Photoelastic material in which different loads are considered such as 55kg, 70kg and 85 kg on disc and the diameter of the disc is 60mm. With the help of material fringe order we can calculate the material fringe value using the formula given below.

$$f\sigma = \frac{8P}{\pi DN}$$

Where- F_6 - Material Fringe Value

D- Diameter of the Disc

D= 60mm

P- Load applied in kg

N- Material fringe order.



Figure.4.1 Calibration of Photoelastic sheet on circular disc.

Table: 4.1. Calibration of Photoelastic sheet

Sr.No.	Applied Load (P) on Material Kg.	Fringe order (N)	Material fringe Value (F_6) (kgf/cm)	Average fringe Value (F_6) (kgf/cm)
01	55	0.80	13.30	13.05
02	70	1.80	12.97	
03	85	2.80	12.89	

Average material fringe value of Photoelastic material is 13.05 kgf/cm.

4.2. Experimentation and Investigation of connecting rod using Photoelasticity

While conducting this stress analysis we get the different fringe pattern on the both ends of connecting rod at different loading condition and we get the different fringe order for different magnitude and at each loading condition with the help of this fringe order we calculated the maximum principle stress at the both ends of connecting rod for both compressive as well as tensile loads.

Maximum principle stress can be calculated using the following formulas

Material fringe value ($F\sigma$) = 13.05N/mm

Model thickness (h) = 6mm

$$\text{Maximum principal stress max } \sigma = \frac{NF\sigma}{h} \text{ N/mm}^2$$

When Compressive and tensile loads of 70kg, 85kg and 100kg is applied on the specimen of connecting rod as shown in the experimental setup and attached connecting rod specimen in figure: 4.2 below



Figure: 4.2 Experimental setup, Compressive and tensile load acting on the both ends of connecting rod specimen.

While conducting this stress analysis we get the different fringe pattern on the both ends of connecting rod at different loading condition and we get the different fringe order for different magnitude and at each loading condition with the help of this fringe order we calculated the maximum principle stress at the both ends of connecting rod for both compressive as well as tensile loads.

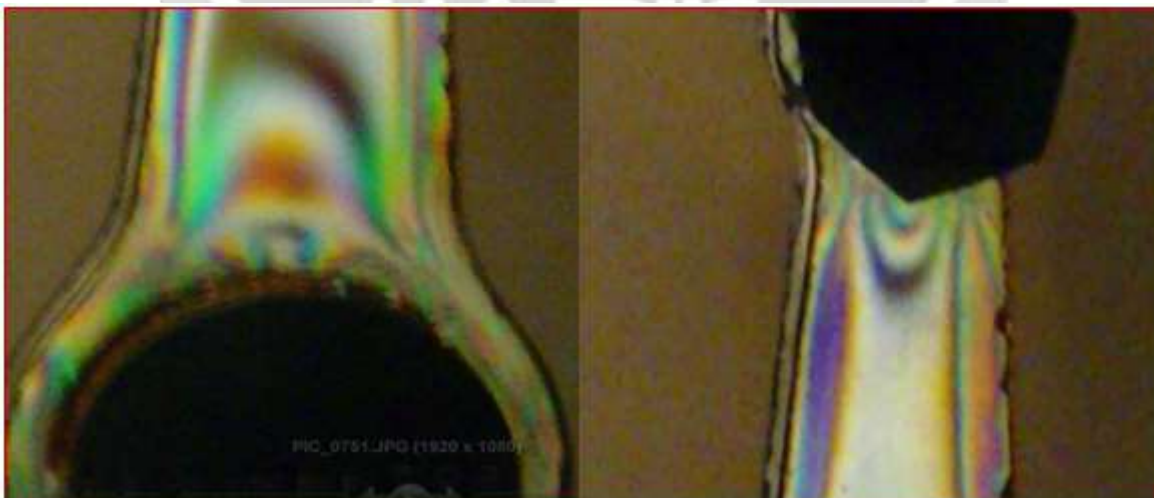


Figure: 4.3 shows the fringes developed on the both end at compressive and tensile load

Table: 4.2. Comparative results of connecting rod specimen experimentally

Sr.no	Load Applied (P) (N)	Maximum Principle Stress at Compressive loading (σ_p) N/mm ²		Maximum Principle Stress at Tensile loading (σ_p) N/mm ²	
		Big End	Small End	Big End	Small End
01	70	5.24	8.85	5.24	8.10
02	85	6.31	10.69	6.31	9.85
03	100	7.47	12.61	7.47	11.60

5.0. CONCLUSIONS

This research work investigated stress analysis of two wheeler connecting rod using Photoelasticity method and using Finite element analysis In this research paper Stress analysis is carried out to find maximum principle stress and reason behind the failure of connecting rod. Following conclusion can be drawn from this study.

[1] It has been observed that tensile stresses are more than compressive stresses at the both ends and there are some considerable differences in the experimental results and the results obtained from finite element analysis are observed.

[2] By observing the different fringes developed in the connecting rod specimen and by calculating the maximum principle stress at that section we can say that the stresses induced in the small end of the connecting rod are greater than the stresses induced at the big end.

[3] From the Photoelasticity analysis it is found that the stress concentration effect exist at both small end and big end and it is negligible in the middle portion of the connecting rod. Therefore, the chances of failure of the connecting rod may be at fillet section of both ends.

[4] While performing the finite element analysis of this connecting rod specimen it is been observed that the maximum stresses are induces at the fillet section of both ends of the specimen and Chances of the failure of the connecting rod is found at the fillet sections of both ends of connecting rod. So to avoid that stresses and failure, material need to be added at the fillet sections of connecting rod.

6.0 ACKNOWLEDGEMENT

I sincerely appreciate **Dr. Dhananjay R Dolas** for accepting me as his student and for giving me the opportunity to work on this research. I am also grateful for his support and guidance that have helped me expand my horizons of thought and expression. Also I would like to thanks our mentor **Dr. Sudhir Deshmukh** principal MGM JNEC Aurangabad and **Dr.M.S.Kadam** Head of the Mechanical department for their valuable cooperation and support for this work.

I would also like to thanks **Dr.B.M.Patil** principal MGM Polytechnic Aurangabad for his understanding, kindness and support toward our research paper.

I also like to thanks **Prof.M.M.Mirza** for providing the valuable inputs during experimentation in their collage in this work and I am very much thankful to Almighty God for giving me the opportunity to enrich my depth of knowledge through research work.

7.0 REFERANCES

- [1] Yoo YM, Haug EJ, Choi KK. Shape optimal design of an engine connecting rod. *J Mech Transom-T ASME* 1984; 106(3):415–419.
- [2] Yang RJ, Dewhirst, DL, Allison JE, Lee A. Shape optimization of connecting rod pin end using a generic model. *Finite Element Analysis Des.* 1992;11(3); 257–264.
- [3] Shenoy PS, Fatemi A. Connecting rod optimization for weight and cost reduction. No. 2005-01-0987. SAE Technical Paper 2005.
- [4] Lapp MT, Krause RA, Hall CC, Dina D, Antic A. Advanced connecting rod design for mass optimization. No. 2010-01-0420. SAE Technical Paper 2010.
- [5] Shenoy PS, Fatemi A. Dynamic analysis of loads and stresses in connecting rods. *Proc Inst Mech Engs, Part C: J Mech Eng. Sci* 2006; 220(5):615–624.
- [6] Ilman MN, Barizy RA. Failure analysis and fatigue performance evaluation of a failed connecting rod of reciprocating air compressor. *Eng. Failure Anal* 2015.
- [7] Moon H, Shin S, Lee K, Chang H, Yeom D. Development and Application of Buckling Estimation Method in Engine Connecting Rod. No. 2007-01-3546. SAE Technical Paper 2007.
- [8] Lee MK, Lee H, Lee TS, Jang H. Buckling sensitivity of a connecting rod to the shank sectional area reduction. *Mats & Des* 2010; 31(6):2796–2803.
- [9] Xu XL, Yu ZW. Failure analysis of a diesel engine connecting rod. *J Failure Anal and Prev* 2007;7(5):316–320.
- [10] Baldini A, Bertocchi E, Giacomini M, Margini S, Rivasi S, Rosi R, Strozzi A. On torsional vibrations in connecting rod assemblies for high performance engines. *SISOM 2007 and Homagial Session of the Commission of Acoustics, Bucharest* 2008; p. 426–432.
- [11] Pioli A, Strozzi A, Baldini A, Giacomini M, Rosi R. Influence of the initial clearance on the peak stress in connecting-rod small ends. *P I Mech Eng. D: J Automobile Eng.* 2009; 223(6):769–782.
- [12] Strozzi A, De Bona F. Hoop stresses in the con-rod small end. *Proc Int Mech Eng. D: J Automobile Eng.* 2005; 219(11):1331–1345.
- [13] Londhe A, Yadav V, Sen A. Finite Element Analysis of Connecting Rod and Correlation with Test. No. 2009-01- 0816. SAE Technical Paper 2009.
- [14] Marmorini L, Baldini A, Bertocchi E, Giacomini M, Rosi R, Strozzi A. On the loosening mechanism of a bush press-fitted in the small end of a connecting rod. *P I Mech Eng. D: J Automobile Eng.* 2011, 0954407011417498.
- [15] Sonsino CM. Fatigue design of sintered connecting rods. *Metal Powder Report* 1990; 45(6):408–412.
- [16] Merritt D, Zhu G. The prediction of connecting rod fretting and fretting initiated fatigue fracture No. 2004-01-3015. SAE Technical Paper 2004..
- [17] Rabb R. Fatigue failure of a connecting rod. *Engine Failure Analysis* 1996; 3(1):13–28.